Comparative Analysis of Various Medical Image Segmentation Techniques

Ayesha Heena[1], Nagashettappa Biradar[2]and Najmuddin M Maroof[3]

Department of Electronics and Instrumentation Engineering[1, 3], Electronics and Communication Engineering[2]

KBNCE, Kalaburgi, INDIA[1, 3], BKIT, Bhalki, INDIA[2]

***E-mail:-** ayeshaheena31@gmail.com[1], nmbiradar@gmail.com[2], ecemaroof99@gmail.com[3]*

DOI: - https://doi.org/10.47531/MANTECH/ECC.2021.32

Abstract

The basic goal in the processing and analysis of echocardiographic images is segmentation. Manually segmented echo images are time-consuming, inconvenient and liable to human subjectivity. There has been a great deal of interest in Computer-Aided Diagnosis (CAD) based or automated segmentation techniques. A lot of work has been done on segmentation techniques in recent years, and numerous studies have been published. In spite of many published studies, the relative merits of the various methods remain unclear. In this paper, a comparative analysis of different segmentation techniques used for medical images in general and echocardiographic images, in particular, is being presented, described, discussed and reviewed. Regarding the utility of these methods, the reasons for the lack of definitive conclusions are explained. Finally, the comparative analysis aims to identify the best within the available segmentation methods and develop a proposed method that can be used for echocardiographic images with promising results.

***Keywords: -** Medical Image Processing, Computer-aided diagnosis, Echocardiographic images, Segmentation techniques*

INTRODUCTION

The quality of data has a strong influence on Medical image segmentation. Due to the characteristic artefacts such as attenuation, speckle, shadows and signal drop out complicates the task of segmentation. Sometimes the orientation dependence of acquisition can result in missing boundaries. The low contrast in areas of interest will increase the complications. In other medical imaging applications, simple image processing can suffice. In the case of ultrasound data, customised methods have proven to be successful.

Automated and semi-automated segmentation techniques are often the most challenging tasks on a great variety of applications. Particularly for diagnostic applications and image-guided interventions, the method of segmentation could accurately delineate contours. The task of segmentation is rather complex due to the relatively low quality of clinical images. Consequently, the reason that motivates the considerable interest in the segmentation of medical images is plenty of approaches for medical image segmentation such as active the contour model expectation maximisation network and learning combined texture and morphological information in various interpretations level sets.

Bayesian techniques

In general, we can classify the methods in two groups of optimisation techniques as offline, which are quite accurate but computationally complex and the fast online algorithms, which are less precise but implementable nearly in real time. Every method has its relevant place in various modalities developed for medical imaging such as Radiography, Computed Tomography (CT), Magnetic Resonance Imaging (MRI), breast thermography, photoacoustic imaging and Ultrasonography. Ultrasonography has a special place even though it provides fewer anatomical details than CT or MRI. Since it has several advantages which make it suitable for numerous applications, its benefits include noninvasive, safe to use and do not cause any adverse effects, inexpensive, quick to perform.

Comparative analyses of ten segmentation methods are carried out with the steps employed in the implementation are shown in fig.1and fig.2.

METHODOLOGY

The most important aspect of this paper is to come up with a suitable segmentation method. A good image segmentation method needs to use all task-specific priors [92],[93], which may be an explicit or implicit assumption in all successful techniques. Due to the relatively low quality of clinical images, methods can be broadly defined in terms of the ones that use imaging physics constraints and the ones that use anatomical shape constraints or temporal constraints or a combination.

The first characteristic feature of clinical images is speckle, which gives the noise like appearance. Speckles inherently exist in images. The local brightness of the speckle pattern does reflect the local echogenicity of the underlying scatterers. Speckle is undesirable and hence seen as noise, which can be reduced. Thus, the segmentation perspective that we chose must remove noise or utilise it for the information contained in it.

We have extensive literature on speckle reduction, which has been proposed as a pre segmentation step. Work includes a Fractional-order integral filter for despeckling of echocardiographic images, wavelet-based methods [1],[2],[3],[4], anisotropic diffusion [5], and many others. [6],[7],[8],[9],[10],[11],[12],[13],[14],[15],[16],[92],[93].

A. Priors

- **Image feature:**

A common method used in Anisotropic diffusion edge detection method is Rayleigh distribution, statistical methods [17], [18],[19],[20],[21],[22] and [23]. In level set method of segmentation Rayleigh distribution was also incorporated [24],[25]. In active contour method and in level set algorithm [30],[31] other Gray level [32],[33],[34],[35],[36],[19],[20],[26],[27],[28][29][39] exponential Gamma and Beta methods a shifted Rayleigh distribution was used.

- **Intensity gradient and higher derivatives:**

In order to find the acoustic discontinuities, the use of intensity gradient as a segmentation constraint is a common practice. Median filtering is used to reduce the effect of noise before gradient estimation [37],[38], also morphological smoothing[39], speckle reduction [40],[41],[42], coarse to fine optimization [32],[3],[6],[34], thresholding basedadaptive smoothing [37],[38] and other pre-processing techniques [43],[44],[45],[46] have been used.

- **Phase:**

To characterize the structures in an image the local phase has been used [47],[48],[49],[50],[51]. Thus, it is possible to characterize intensity features in terms of shape. Thus, phase is more robust feature for boundary detection. Phase is generally estimated using quadrature filter banks. We can also find a link between wavelet-based methods and phase-based methods.

- **Similarity measures:**

The abovementioned has been used to provide an estimate in spatiotemporal analysis and the segmentation feature of almost all Ultrasound image segmentation. The intensity prior will be considered in the segmentation process using the similarity measure.

- **Texture measure:**

Texture in images depends intrinsically on the imaging system. Imaging system physics independent patterns of intensities form the basis for texture measures [52],[53]. The goal of segmentation is to characterise the objects present in the image rather than their actual physical properties. The texture analysis methods have proven to be successful. So, texture-based segmentation algorithms have been proposed and used in various clinical applications. [54] echocardiography.

- **Shape:**

Edges, regions and boundary information may not be sufficient for reliable and accurate segmentation. Rather shape constraints are often effective in improving results. The shape is a constraint that have proved to be popular and successful in all Ultrasound image segmentation [55],[56],[57],[58],[59],[60],[61],[62],[63],[64],[93].

In segmentation methods, information of shape is often embedded. The most classical shape constraint is considered to be boundary regularisation in active contour. We can impose shape constraints [59] by using learned distributions of the shape parameter over a set of training examples. The shape constraint can be imposed by restricting with a set of transformations that does not require training. The Point Distribution Model (PDM) [64] is the most widely used method of employing a shape constraint, which describes average shape and shape variations of a set of training samples using principal component analysis (PCA). PDM segmentation is known as the active shape model (ASM), which are more suitable to describe free

form transformations. The active appearance model (AAM) is an extension to intensity prior information was proposed [65], another extension is the inclusion of motion information [66] and extension of AAM to 3D was proposed later [68] AAM approach could be used to address both the geometric shape and boundary model. The only limitation of AAM is it assumes a similar appearance of clinical images from different subjects. Since there are subject to subject tissue property variations, operator to operator variations during acquisition make it challenging to achieve routine clinical images. Bosch et al. [68], Leventon et al. [67] proposed a nonlinear normalisation step to reduce these effects. They proposed to use a level set representation of shape to overcome point to point correspondence limitation in the learning stage. However, the shape model is only as good as training samples. We can use it as a model framework. The aptitude of shape constraints is still an important issue of consideration.

- **Time:**

Echocardiographic images, or all Ultrasound images, are generally employed in real time, so the data available for segmentation is a temporal image sequence rather than a static frame. It becomes essential to use temporal priors in the spatiotemporal segmentation process, particularly in echocardiographic segmentation where the motion is periodic. The introduction of unwanted motion is due to respiration. The only way to deal with motion is before segmentation when we register the data. Sometimes correction or estimation can also be considered in the segmentation process via temporal prior. Hence there are various forms of temporal priors. It depends on parameterisation done on the motion and whether the segmentation method's designing has the determining factor of required computation speed. Few authors have considered the space parameters to be treated differently from time parameters [5], while others have added time as an extra-dimensional segmentation problem [68]. There is a need for a better understanding of the strengths and limitations of segmentation methods through comparisons to validate the type of segmentation and databases available as ideally standard databases. Even though Ultrasound and echocardiography, in particular, are widely used in clinical diagnosis and image-guided interventions, this field is far behind the other areas of clinical image analysis. We have also emphasised in the methodology section that segmentation methods should utilise priors. But for generic image segmentation, the choice of these constraints is application-specific.

B. Comparison of the segmentation of B-Mode, Continuous wave Doppler (CWD), Color Doppler (CD) images and synthetic test images with intensity inhomogeneity is carried out in the paper. The segmentation techniques employed were based on concepts of edge, region, watershed [71], fuzzy and active contour [72] and Chan Vese [69],[70]. The images acquired in two parasternal and three apical views along with CWD and CD images [73],[74],[75],[76],[78] were used in the analysis of segmentation techniques, which highlighted the importance of integrated analysis Multiview images. An overview of segmentation techniques analysed for CWD, B-Mode and CD images are tabulated in Table 1. These methods are employed in the delineation of various types of images with intensity inhomogeneity and low contrast. The methods depicted in Fig 1 and 2 employed for delineation of the outer boundaries of the CWD spectrum are described. These methods were advocated for segmentation of images such as MRI, CT and synthetic images.

1. Magagnin method: Magagnin et al. [75] had proposed a semi-automatic segmentation method. The fundamental steps of this technique are shown in Fig 1 as Method 1

2. Wavelet-based scale multiplication edge detection (SMED) was advocated by Bao et al. [83] to improve edge detection accuracy in synthetic and natural images. It could be a method for outer boundary detection in echocardiographic images. The fundamental steps of this technique are shown in Fig 1 as Method 2. The approach includes the estimation of a threshold at each scale and wavelet transform of the input image. The steps employed consist of computing the thresholds and estimating the correlation between the pixels. The correlation between pixels row-wise and column-wise are calculated on the application of wavelet transform. Before estimating correlation, the wavelet coefficients are thresholded. This is followed by the construction of the modulus matrix and direction estimation. The estimated pixels in various directions are subjected to nonminimum suppression. The resultant image is filtered for the suppression of noise. The boundaries are traced and superimposed on the original image. Details of the SMED method & its implementation steps are brought out in [83].

3. Charia and Ray [84] proposed a distance measure called intuitionistic fuzzy divergence (IFD) for edge detection in brain image, Rice

image, lung image Aorta image and cameraman images. IFD based edge detection [82]is employed to trace echocardiographic images' boundaries since it was based on hesitation degree, non-membership degree and membership degree. The approach consists of the formation of sixteen templates initialisation, finding the hesitation degree, estimation of the maximum divergence transforming fuzzy domain image into pixel domain, thresholding and morphological operators [89],[81],[84],[82]. All these steps are shown in Fig 1. Chaira and Ray [84] provided the step-wise details of this approach. The method is referred to as Method 3 in Fig 1. The significant effects of IFD techniques are (i) formation of the edge detected templates (ii) Application of edge template over the image (iii) Computation of IFD between each element of every template and the image window (iv) Selection of the maximum of template among the minimum IFD values (v) Positioning of the maximum values (vi) Selection of positioning of max-min value (vii) Construction of new divergence matrix (viii) Thresholding of divergence matrix and obtain edge detected image.

4. A fuzzy soft thresholding approach based on fuzzy aggregation methods were proposed for the medical images by Aja Fernandes et al. [85]. The core idea of soft thresholding was to relate each image pixel with others in terms of fuzzy membership functions. These membership functions are derived from histograms of various regions in the image. Each of the pixels would thus belong to multiple regions with different membership functions. Therefore, the pixels are segregated from the noisy ones easily in any given noisy image. These segregation methods are employed for the segmentation of echocardiographic images, which are inherent with speckle noise. The steps used in the implementation of these methods are shown in Fig 1. Every pixel is correlated to other pixels in various image parts using fuzzy membership functions instead of a hard decision like wavelet-based thresholding. The fuzzy C-Means (FCM) clustering is employed for sorting the pixels followed by computation of the pseudo trapezoidal-shaped membership functions. Various aggregation approaches such as maximum. Median, recursive average aggregation and absolute maximum aggregation were employed in experimentations. This method is referred to as Method 4 in Fig 1.

Table 1 Overview of Segmentation Techniques for B-Mode, Cwd and Color Doppler Images

Ref	Year	Type	Abbrevia tion	Expansion	Application of the Method
[195]	2006	Edge	Magagnin	Magagnin Method	Pulsed Doppler Images
[287]	2005	Edge	SMED	Scale Multiplication	Synthetic and Natural
[288]	2008	Fuzzy	IFD	Intuitionistic fuzzy divergence	CT and standard Images
[289]	2010	Fuzzy	FTS	Fuzzy soft threshold	Head MRI, XRay, TTE.
[46, 289]	2005	Topologica l Derivative	DTD	Discrete Topological Derivative	CTAngiography, head MRI
[199]	2006	Edge	Kiruthika	Edge Based Segmentation	CW-Doppler images.
[184]	2013	Level Set	RD	Reaction Diffusion	Synthetic and MRI Image
[184]	2013	Level Set	GDRLSE1	Generalized Distance Regularized Level set Evolution.	Synthetic and MRI Image
[184]	2013	Level Set	GDRLSE2		Synthetic and MRI Image
[184]	2013	Level Set	GDRLSE3		Synthetic and MRI Image
[154]	2008	Level Set	RSF	Region Scalable Fitting	Brain MR , Vessel Image
[304]	2010	Active Contour	LIF	Local Image Fitting Energy	Synthetic and MRI Image
[292]	2011	Level Set	LSEBFE	Intensity In homogeneities	CT Image of Vessel
[293]	2010	Active Contour	IVC	Regularized Level Set	MRI
[183]	2007	Active Contour	GMAC	Global Minimization of Active Contour	Synthetic Images
[294]	2009	Active Contour	LFE	Laplacian Fitting Energy	Synthetic Images
[175]	2010	Level Set	SVMLS	Multiphase Level Set.	MRI image
[295]	2007	Clustering	FCM	Fuzzy C-Means.	US Carotid Artery
[25,296, 297]	2009 - 2011	Region	Region	Region Growing	Ultrasound Images, Weld images.
		Edge	Adaptive Canny	Canny Edge detection	
		Watershed	Multiwater	Multi stage water shed	

5. Topological derivative-based segmentation, the topological sensitivity provides information of the edges in the image and derivative speaks about the incremental changes in topology Larrabide et al. [86] had advocated this technique to overcome iterative processing of images during segmentation. The method was tested for segmentation of CT and MRI. This segmentation method was analysed for tracing the outer boundaries of the echocardiographic images acquired in multiple views from patients diagnosed with Aortic Regurgitation [77],[79],[80]. The major steps of the topological derivative based segmentation are shown in Fig 1. The images are normalised, and an initial guess is made regarding the class of images. The total variation of the initial guess computed, followed by the application of a fixed-point algorithm. The pixels with negative topological derivatives are traced. A class is formed with smaller values of each of the pixels. The class is optimised, resulting in the required segmented image. The total variation for the segmented image is estimated, and the original intensities are restored. This method is referred to as Method 5 in Fig 1.
6. Segmentation using histogram equalisation. The histogram equalisation enhances the image's contrast by redistributing the Gray values equally over the entire image. It enhances the contrast for values close to histogram maxima and decreases contrast near minima [89],[90]. The histogram equalisation homomorphic filter and Canny edge detection were employed for tracing the outer boundaries of the echocardiographic CWD images. The brightness levels of the image are equally distributed for full scale by using MATLAB function "histeq". The enhanced images are filtered using the homomorphic filter. On application of filtering, the image's contrast is reduced and to compensate for this, adaptive contrast enhancement is performed. The enhancement is based on the difference between each pixel value and its deviation. The enhanced images are filtered using a median filter with a window size of 7x7. The edges in the image are detected using Canny edge detection. The obtained boundaries have discontinuities and unwanted objects connected to the boundary, addressed using morphological operations such as dilation and erosion. The resultant image is superimposed on the enhanced image. The steps incorporated in the algorithm are shown in Fig 2 for quick reference and better understanding. This method is referred to as Method 6 in Fig 2.

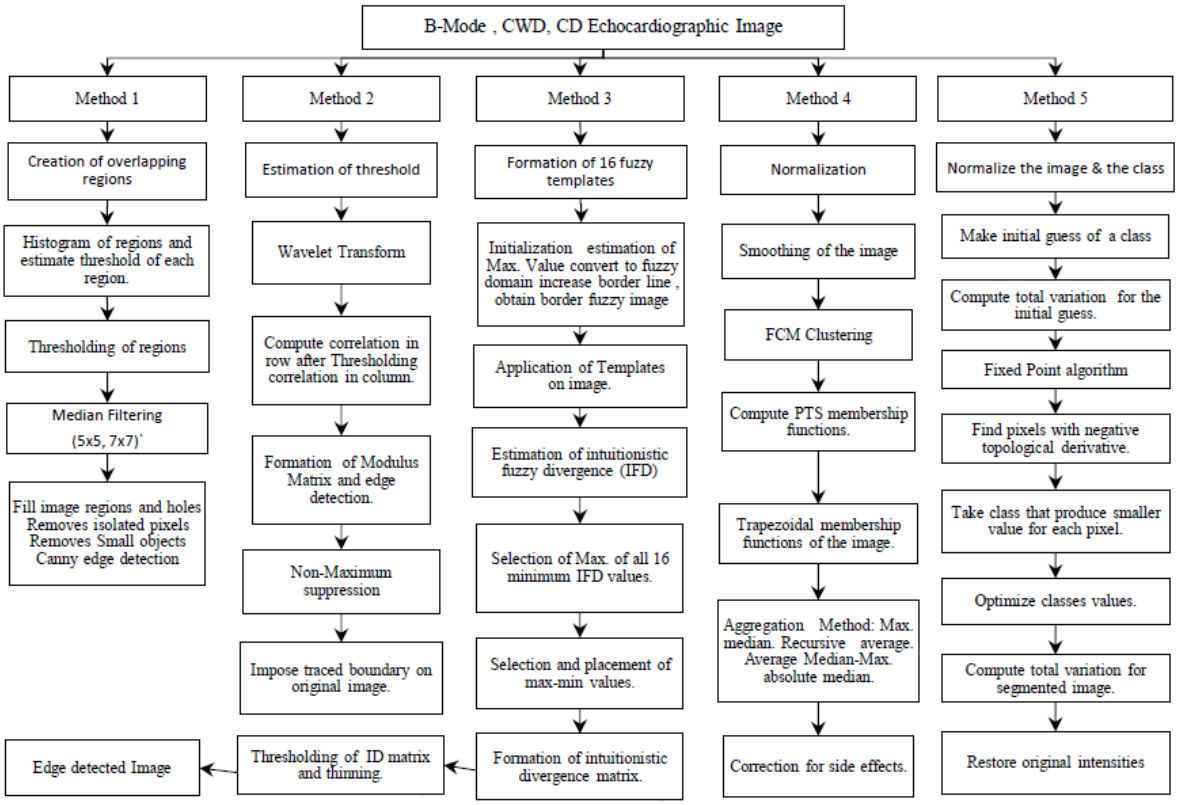

Fig. 1: Segmentation techniques for B-Mode, CWD and CD images –Method 1 to Method 5

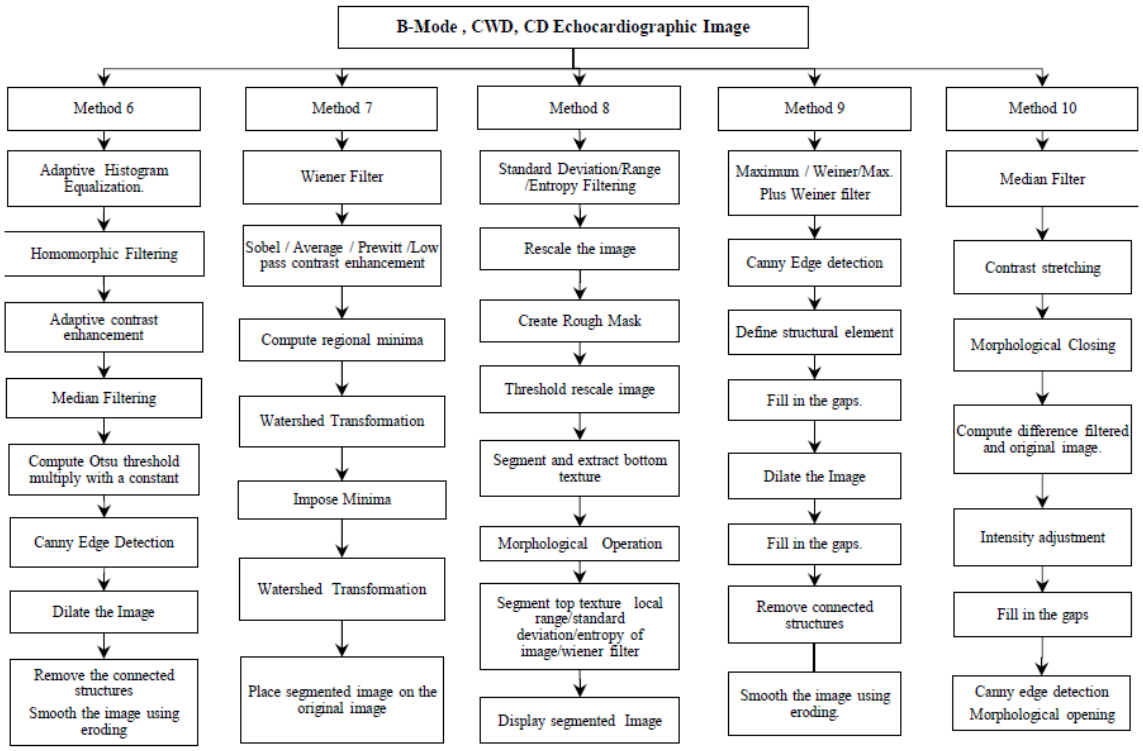

Fig. 2: Segmentation techniques for B-Mode, CWD and CD images –Method 6 to Method 10

7. Multistage watershed transforms based segmentation. It comes under the family of the region-based segmentation. It is based on mathematical morphology. This technique combines concepts of thresholding, detection of discontinuities and region processing. The advantage of using watershed is when employed on another level will assist in forging the fragmented regions [86],[87],[88]. Some of the essential steps in this method of segmentation are the images need to be converted into greyscale and resized to 512x512. These images are pre-processed using an adaptive Wiener filter employing the MATLAB function "wiener2". The pre-processed image is then employed to compute the gradient where various gradient operators such as Sobel, Prewitt, Roberts or Gaussian derivatives are used. The gradient image is subdivided into initial regions employing gradient magnitude.

8. The edges so obtained are grouped to form contour. The initial watershed may result in many smaller regions, often reflecting over-segmentation or generating undesired smaller regions. The boundaries within the homogeneous region are weaker. The neighbourhood relation is in terms of the connectivity graph from the image. The thresholded image is converted into a binary image. The morphological operations and watershed top head transformation are employed to compute the bright objects present in the image. The peak values which significantly differ from the local background are estimated. The partially overlapping regions are separated using the watershed. The smaller objects are weeded out using morphological operations. The Euclidean distance map (EDM) is computed for the resultant image. The resultant labelled image is eroded to match the content and background borders. This region provided a Region of interest ROI with the boundaries marked. The smaller regions with some homogeneous intensity characteristics are merged. Thus, the multistage watershed transform-based segmentation provided better tracing than edge and region growing based segmentation.

9. Segmentation using texture filters. The texture-based filters play an important role in the boundary detection of the images [91],[92]. The three texture filters available in MATLAB are "stdfilt", "rangefilt", and "entropyfilt" employed for CWD image segmentation. The steps employed in the implementation of texture-based segmentation are shown in Fig 2 as Method 8. This method is implemented in two stages.

10. Segmentation using the adaptive and maximum filter: The combination of maximum filter, adaptive Wiener and Canny edge detection are employed to segment CWD

images. The CWD images are denoised using the combination of maximum and adaptive Wiener filters. Implementation steps of this approach are shown in Fig 2 as Method 9. The despeckled images are subjected to Canny edge detection and morphological operations for tracing the outer boundaries. The other edge detection techniques such as Sobel, Prewitts and Roberts were also tested. It was observed that performance using Canny edge was better; hence results based on this were better. The sequential combination of adaptive Wiener and maximum filter followed by Canny edge detection stood out. The morphological operations are performed for the reasons already discussed in watershed-based segmentation.

11. Kiruthika method of segmentation. Kiruthika et al. [78] had proposed a method for tracing out boundaries of the CWD images acquired during Aortic regurgitation. This method employed the combination of median filter, contrast enhancement, Gaussian filter, morphological operations, intensity adjustments, and Canny edge detection to trace the CWD spectrum's outer boundaries. The adaptive Wiener filter's performance was superior to Gaussian in terms of speckle-noise suppression and edge preservation. The necessities of Gaussian filter after contrast enhancement could overcome the problem. The images were initially filtered using median filter followed by Wiener filter. Then the images were processed using morphological closing operation, and then intensities were adjusted using inbuilt function "imadjust" and "imfill" operations. The edges in the resultant images were obtained using Canny edge detection, combined with the morphological opening operation. Finally, the output image was superimposed on the enhanced image. The steps employed are shown in Fig 2 as Method 10.

A. K-nearest neighbor method for segmentation:

The K-nearest neighbours (KNN) algorithm is a unique, user-friendly approach with a wide range of applications, including machine learning algorithms which are majorly used for the various image processing applications, including classification, segmentation and regression issues of image processing. On the other hand, it is an efficient algorithm that can be implemented easily as per the user needs. Still, with the limiting factor, the computational speed is significantly less when the number of data sets increases, which also interprets the computational speed, is quite high for the fewest number of data for the processing.

This KNN algorithm operates with the basic principle of the number of weights or the calculated distance among the query and the selective examples in the data set by the specific number, a variable defined as 'K', and this 'K' is the closest among the query. The selection will be made on the relevant frequency label of the data to classify pixels in the image data, or it identifies the average labels for the regression operations. In the regression-based operation, it can be quoted that the selection of the suitable 'K' for the required data serve for the best of the 'K' states which will be the best one for the exchange and selection of pixel data. In contrast, the KNN algorithm is the best for query and processing.

A weighted directed graph is a perfect term to define the KNN graph. In this graph, every node is represented by a cluster and the edge of each pointer to the neighbour cluster if we consider that each node has K adjust, then also having K nearest clusters.

Classification of the images in medical imaging is very important. KNN is one suitable algorithm technique that is simple. It is conceptual and computational, which provides excellent accuracy in classification. The algorithm KNN is based on the distance function voting.

The Contrast, when the scale of local texture is larger the distance

$$C=\Sigma k2\Sigma M(i,j)|i-j|=km-1k=0. \quad (1)$$

k->neighboring pixels

Homogeneity is represented as

$$H=\Sigma\Sigma(M(i,j)))2ji\,. \quad (2)$$

Entropy is the measure of randomness: close to either 0 or 1

$$E=\Sigma\Sigma(M(i,j))\log(M(i,j))ji \quad (3)$$

Local Homogeneity (LH) is given as

$$LH=\Sigma\Sigma_{M\,(i,j)1+(i-j)2ji}. \quad (4)$$

The aforementioned four features/parameters of the medical image given in equations 1,2,3,4 are essential for the KNN based image segmentation, which will be done at the pixel level for the query and reference pixel. In this regard, the first parameter contrast is given by equation (1), in which the texture decision is made on the difference of the test image with the neighbouring pixels. The secondary parameter is homogeneity, which decides the pixel region and background

image, which is not our concern. On the other hand, it is most required for the data extraction from the region of interest to the medical image data, given by the equation (2). The following parameter is the entropy provided by equation (3), in which it plays a decision parameter for the 1 or 0 for pixel exchange. The last parameter, Local Homogeneity, which is similar to the homogeneity, is done among the inter and intra pixel analysis given by equation (4).

The KNN based approach for the segmentation can be listed into four different phases, namely:

- Pre-Processing
- Feature extraction
- Classification
- Post processing
- Post processing

Phase 1: Pre-processing

The removal of noise and the conversion of the image to grayscale is completed in the process of pre-processing.

The median filter is used here.

The median filters have the following advantages:

1. The contrast in the steps is not reduced.
2. The boundaries are not shifted in the median filtering.
3. The median filtering is not affected by the outliers.

Phase 2: Feature Extraction

The main intention of feature extraction is to reduce the original set of databases that are distinguishable on the input patterns. Haralick's texture feature extraction method extracts features such as correlation, Homogeneous, entropy, contrast and local Homogeneous.

Phase 3: classification

The pixels are classified into similar classes by the training data, which has the same level of intensity. This classification is done in the nearest neighbourhood algorithm. To avoid the errors that occur because of the single neighbourhood outliner of other classes and improves the robustness of the approach, the classifier works with k patterns [94-103]. Hence, it is called K nearest neighbourhood algorithm.

The KNN algorithm has the following:

1. Classes are Included in training set
2. The items to be classified are examined towards the k term.
3. Most of the closed items are placed near the new item.
4. O(q) for each tuple to be classified.

Phase 4: Post Processing

The extraction of abnormal region from the echo image is done in the step of post processing. Firstly, the removal of cult involves removal of Grey matter and hence the abnormal region extracted segmented image is obtained with the KNN. The results of the KNN algorithm are shown in Fig 3.

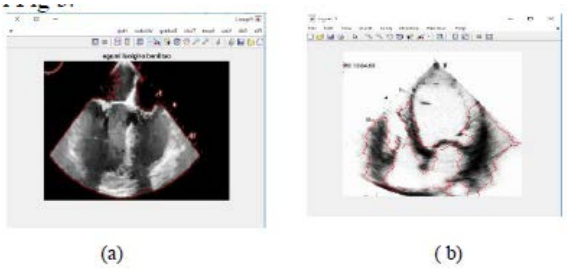

Fig. 3 (a) original image with contour marked. (b) Segmented image with the KNN

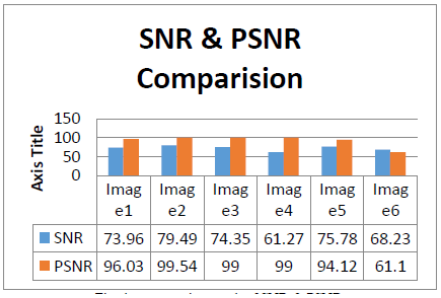

Fig. 4: Comparative graph of SNR & PSNR

It should also be noted that the developed algorithm can also be applied to any of the real time or other untrained databases for the applications. An advanced algorithm can be designed for video applications, satellite images, and other image formats as a future enhancement. The next improvement can also be extended to the comparative analysis among other available database.

CONCLUSION

Of the various methods discussed in the comparative analysis of the paper, Method 9 and Method 10 stand out in performance. The algorithm developed is processed with the G-L based algorithm for denoising and combined with the KNN based segmentation.

The algorithm is better than the existing methods, with various standard medical images and other image databases. The desired algorithm is also tested with the non-medical image database, and its comparative analysis is done with the existing and proposed algorithms. The standard image

database for the various analysis is described by calculating SNR & PSNR, as shown in figure 4.

REFERENCES

1. Achim, A. Bezerianos, and T. P., “Novel Bayesian multi-scale method for speckle removal in medical ultrasound images,” IEEE Trans. Med. Imaging, vol. 20, no. 8, pp. 772–783, Aug. 2001. [
2. S. Gupta, R. C. Chauhan, and S. C. Saxena, "Wavelet-based statistical approach for speckle reduction in medical ultrasound images," MBEC, vol. 42, pp. 189–192, 2004.
3. X. Zong, A. F. Laine, and E. A. Geiser, “Speckle reduction and contrast enhancement of echocardiograms via multi-scale nonlinear processing,” IEEE Trans. Med. Imaging, vol. 17, no. 4, pp. 532–540, Aug. 1998.
4. C.-Y. Xiao, S. Zhang, and Y.-z. Chen, “A diffusion stick method for speckle suppression in ultrasonic images,” Pattern Recognit. Lett., vol. 25, no. 16, pp. 1867–1877, Dec. 2004.
5. K. Mikula, T. Preußer, and M. Rumpf, "Morphological image sequence processing," Computing and Visualisation in Science, vol. 6, no. 4, pp. 197–209, 2004.
6. A. Ashton and K. Parker, “Multiple resolution Bayesian segmentation of ultrasound images,” Ultrasonic Imaging, vol. 17, no. 4, pp. 291–304, Oct. 1995.
7. Y. Yu and S. T. Acton, “Speckle reducing anisotropic diffusion,” IEEE Trans. Image Process., vol. 11, no. 11, pp. 1260–1270, Nov. 2002.
8. K. Z. Abd-Elmoniem, A.-B. M. Youssef, and Y. M. Kadah, "Real-time speckle reduction and coherence enhancement in ultrasound imaging via nonlinear anisotropic diffusion," IEEE Trans. Biomedical Engineering, vol. 49, no. 9, pp. 997–1014, 2002.
9. K. Krissian, K. Vosburgh, R. Kikinis, and C.-F. Westin, “Anisotropic diffusion of ultrasound constrained by speckle noise model,” Laboratory of mathematics in imaging, Harvard Medical School,” Technical Report, 2004. [
10. Tauber, H. Batavia, and A. Ayache, "A robust speckle reducing anisotropic diffusion," in IEEE Int. Conf. Image Proc., vol. 1, Singapore, 2004, pp. 247– 250.
11. A. N. Evans and M. S. Nixon, “Biased motion-adaptive temporal filtering for speckle reduction in echocardiography,” IEEE Trans. Med. Imaging, vol. 15, no. 1, pp. 39–50, Feb. 1996.
12. M. Karaman, M. A. Kutay, and G. Bozdagi, “Adaptive speckle suppression filter for medical ultrasonic imaging,” IEEE Trans. Med. Imaging, vol. 14, no. 2, pp. 283–292, June 1995.
13. Avianto and M. Ito, “Speckle reduction for ultrasonic images using fuzzy morphology,” IEICE Trans. Inf. Syst., vol. E84-D, no. 4, pp. 502– 510, Apr. 2001.
14. V. H. Metzler, M. Puls, and T. Aach, "Denoising of ultrasound sector scan by nonlinear filtering of a morphological and linear ratio pyramid," in Medical Imaging 2001: Image Processing, M. Sonka andK. M. Hanson, Eds., vol. 4322, no. 1. San Diego, CA, USA: SPIE, 2001, pp. 480–491.
15. M. Ito, M. Tsubai, and A. Nomura, “Morphological operations by locally variable structuring elements and their applications to region extraction in ultrasound images,” Syst. Comput. Japan, vol. 34, no. 3, pp. 33–43, Feb. 2003.
16. T. Eltoft, “Speckle: Modeling and filtering,” in Norwegian Signal Processing Symposium, Bergen Norway, 2-3Oct. 2003.
17. R. N. Czerwinski, D. L. Jones, and W. D. O’Brien, Jr., “Detection of lines and boundaries in speckle images – application to medical ultrasound,” IEEE Trans. Med. Imaging, vol. 18, no. 2, pp. 126–136, Feb. 1999.
18. E. Steen and B. Olstad, “Scale-space and boundary detection in ultrasound imaging, using signal-adaptive anisotropic diffusion,” in Proc. SPIE Medical Imaging: Image Processing, 1994.
19. N. Paragios, M. P. Jolly, M. Taron, and R. Ramaraj, “Active shape models & segmentation of the left ventricle in echocardiography,” in Int. Conf. Scale Space Theories and PDEs methods in Computer Vision, ser. Lect. Note Comput. Sci, vol. 3459, 2005, pp. 131–142.
20. N. Lin, W. C. Yu, and J. S. Duncan, "Combinative multi-scale level set framework for echocardiographic image segmentation," in MICCAI, ser. Lect. Note Comput. Sci, vol. 2488, Tokyo, Japan, 2002, pp. 682– 689.
21. Shao, K. V. Ling, and W. S. Ng, “Automatic 3D prostate surface detection from TRUS with level sets,” Int. J. Image Graphics, vol. 4, no. 3, pp. 385–403, July 2004.
22. Z. Tao, C. C. Jaffe, and H. D. Tagare, “Tunnelling descent: A new algorithm for active contour segmentation of ultrasound images,” in Info. Proc. Med. Imaging, ser. Lect. Note Comput. Sci, vol. 2732, Ambleside, UK, 2003, pp. 246–257.
23. E. Brusseau, C. L. de Korte, F. Mastik, J. Schaar, and A. F. W. van der Steen, “Fully automatic luminal contour segmentation in

intracoronary ultrasound imaging – A statistical approach," IEEE Trans. Med. Imaging, vol. 23, no. 5, pp. 554–566, May 2004.

24. Haas, H. Ermert, S. Holt, P. Grewe, A. Machraoui, and J. Barmeyer, "Segmentation of 3D intravascular ultrasonic images based on a random field model," Ultrasound Med. Biol, vol. 26, no. 2, pp. 297– 306, Feb. 2000.
25. F. Gue´rault, P. Delachartre, G. Finet, and I. E. Magnin, "Modelization and segmentation of intravascular ultrasound images," Traitement du Signal, vol. 17, no. 5-6, pp. 517–533, 2000
26. S. M. G. V. B. Jardim and M. A. T. Figueiredo, "Segmentation of fetal ultrasound images," Ultrasound Med. Biol, vol. 31, no. 2, pp. 243–250, 2005.
27. M. A. Figueiredo, J. M. N. Leita˜o, and A. K. Jain, "Unsupervised contour representation and estimation using B-splines and a minimum description length criterion," IEEE Trans. Med. Imaging, vol. 9, no. 6, pp. 1075–1087, June 2000.
28. A. Sarti, E. Mazzini, C. Corsi, and C. Lamberti, "Maximum likelihood segmentation of ultrasound images with Rayleigh distribution," IEEE Trans. Ultra. Fer. Freq. Control, vol. 52, no. 6, pp. 974–960, June 2005.
29. M. J. Ledesma-Carbayo, J. Kybic, M. Desco, A. Santos, M. S´'uhling, P. Hunziker, and M. Unser, "Spatiotemporal non-rigid registration for ultrasound cardiac motion estimation," IEEE Trans. Med. Imaging, vol. 24, no. 9, Sept. 2005
30. M.-H. R. Cardinal, J. Meunier, G. Soulez, E. Thrasse, and G. Cloutier, "Intravascular ultrasound image segmentation: A fast-marching method," in MICCAI, ser. Lect. Note Comput.sci. Canada, 2003, pp. 432–439
31. Baillard and C. Barillot, "Robust 3D segmentation of anatomical structures with level sets," in MICCAI, ser. Lect. Note Comput. Sci, vol. 1935, Pittsburgh, Pennsylvania, USA, 2000, pp. 236–245. [
32. Boukerroui, A. Baskurt, J. A. Noble, and O. Basset, "Segmentation of ultrasound images - multiresolution 2D and 3D algorithm based on global and local statistics," Pattern Recognit. Lett., vol. 24, no. 4-5, pp. 779–790, Feb. 2003.
33. M. B. Hansen, J. Moller, and F. A. Togersen, "Bayesian contour detection in a time series of ultrasound images through dynamic deformable template models," Biostatistics, vol. 3, no. 2, pp. 213–228, June 2002.
34. Boukerroui, O. Basset, A. Baskurt, and G. Gimenez, "A multiparametric and multi resolution segmentation algorithm of 3-D ultrasonic data," IEEE Trans. Ultra. Fer. Freq. Control, vol. 48, no. 1, pp. 64–77, Jan. 2001.
35. M. J. Ledesma-Carbayo, J. Kybic, M. Desco, A. Santos, M. S´'uhling, P. Hunziker, and M. Unser, "Spatio-temporal non-rigid registration for ultrasound cardiac motion estimation," IEEE Trans. Med. Imaging, vol. 24, no. 9, Sept. 2005.
36. M. Martin-Fernandez and C. Alberola-Lopez, "An approach for contour detection of human kidneys from ultrasound images using Markov random fields and active contours," Med. Image Anal., vol. 9, pp. 1–23, 2005.
37. A. Krivanek and M. Sonka, "Ovarian ultrasound image analysis: Follicle segmentation," IEEE Trans. Med. Imaging, vol. 17, no. 6, pp. 935–944, Dec. 1998.
38. A. Potocˇnik and D. Zazula, "Automated analysis of a sequence of ovarian ultrasound images. Part I: segmentation of single 2D images," Image Vis. Comput., vol. 20, pp. 217–225, 2002.
39. Mishra, P. K. Dutta, and M. K. Ghosh, "A GA based approach for boundary detection of the left ventricle with echocardiographic image sequences," Image Vis. Comput., vol. 21, pp. 967–976, 2003.
40. L. X. Gong, S. D. Pathak, D. R. Haynor, P. S. Cho, and Y. Kim, "Parametric shape modelling using deformable super ellipses for prostate segmentation," IEEE Trans. Med. Imaging, vol. 23, no. 3, pp. 340–349, Mar. 2004.
41. S. D. Pathak, V. Chalana, D. R. Haynor, and Y. Kim, "Edge-guided boundary delineation in prostate ultrasound images," IEEE Trans. Med. Imaging, vol. 19, no. 12, pp. 1211–1219, Dec. 2000 [
42. Y. Yu, J. A. Molloy, and S. T. Acton, "Segmentation of the prostate from supra-pubic ultrasound images," Med. Phys., vol. 31, no. 12, pp. 3474–3484, Dec. 2004.
43. Sahiner, H. P. Chan, M. A. Roubidoux, M. A. Helvie, L. M. Hadjiiski, A. Ramachandran, C. Paramagul, G. L. LeCarpentier, A. Nees, and C. Blane, "Computerised characterisation of breast masses on three-dimensional ultrasound volumes," Med. Phys., vol. 31, no. 4, pp. 744–754, Apr. 2004.
44. R. G. Aarnink, R. J. B. Giesen, A. L. Huynen, J. J. M. C. H. de la Rosette, F. M. J. Debruyne, and H. Wijkstra, "A practical clinical method for contour determination in ultrasonographic prostate images," Ultrasound Med. Biol, vol. 20, pp. 705–717, 1994.
45. A. Takagi, K. Hibi, X. Zhang, T. J. Teo, H. N. Bonneau, P. G. Yock, and P. J. Fitzgerald, "Automated contour detection for high-frequency intravascular ultrasound imaging: a

technique with blood noise reduction for edge enhancement," Ultrasound Med. Biol, vol. 26, pp. 1033–1041, 2000.

46. A. J. Bouma, W. J. Niessen, K. J. Zuiderveld, E. J. Gussenhoven, and M. A. Viergever, "Automated lumen definition from 30 MHz intravascular ultrasound images," Med. Image Anal., vol. 1, pp. 363– 377, Sept. 1997.
47. M. Mulet-Parada and J. A. Noble, "2D+T acoustic boundary detection in echocardiography," Med. Image Anal., vol. 4, no. 1, pp. 21–30, Mar. 2000.
48. M. Mulet-Parada, "Intensity independent feature extraction and tracking in echocardiographic sequences," PhD dissertation, Department of Engineering Science, University of Oxford, UK, 2000.
49. Boukerroui, J. A. Noble, M. C. Robini, and M. Brady, "Enhancement of contrast regions in suboptimal ultrasound images with application to echocardiography," Ultrasound Med. Biol, vol. 27, no. 12, pp. 1583– 1594, Dec. 2001.
50. X. Ye, J. A. Noble, and D. Atkinson, "3-D freehand echocardiography for automatic left ventricle reconstruction and analysis based on multiple acoustic windows," IEEE Trans. Med. Imaging, vol. 21, no. 9, pp. 1051–1058, Sept. 2002.
51. Sanchez-Ortiz, G. Wright, J. Declerck, A. Banning, and J. Noble, "Automated 3D echocardiography analysis compared with manual delineations and SPECT MUGA," IEEE Trans. Med. Imaging, vol. 21, no. 9, pp. 1069–1076, Sept. 2002.
52. M. Tuceryan and A. K. Jain, The Handbook of Pattern Recognition and Computer Vision, Chen C. M. et al. ed. World Scientific Publishing Co., 1998, ch. Texture Analysis, pp. 207–248. [
53. Y. Rolland, J. Bezy-Wendling, H. Gestin, A. Bruno, R. Duvauferrier, N. Morcet, R. Collorec, and J. L. Coatrieux, "Analysis of texture in medical imaging. Review of the literature," Ann Radiol (Paris), vol. 38, no. 6, pp. 315–347, 1995
54. T. Binder, M. Sussner, D. Moertl, H. Strohmer, T Baumgartner,G. Maurer, and G. Porenta, "Artificial neural networks and spatial, temporal contour linking for automated endocardial contour detection on echocardiograms: A novel approach to determine left ventricular contractile function," Ultrasound Med. Biol, vol. 25, no. 7, pp. 1069– 1076, Sept. 1999.
55. J. G. Bosch, S. C. Mitchell, B. P. F. Lelieveldt, F. Nijland, O. Kamp,M. Sonka, and J. H. C. Reiber, "Automatic segmentation of echocardiographic sequences by active appearance motion models," IEEE Trans. Med. Imaging, vol. 21, no. 11, pp. 1374–1383, Nov. 2002.
56. Y. Chen, H. Tagare, S. Thiruvenkadam, F. Huang, D. Wilson, K. S. Gopinath, R. W. Briggs, and E. A. Geiser, "Using prior shapes in active geometric contours in a variational framework," Int. J. Comput. Vis., vol. 50, no. 3, pp. 315–328, Dec. 2002.
57. Y. Chen, F. Huang, H. D. Tagare, M. Rao, D. Wilson, and E. A. Geiser, "A coupled minimisation problem for medical image segmentation with priors," Int. J. Comput. Vis., vol.
58. S. C. Mitchell, J. G. Bosch, B. P. F. Lelieveldt, R. J. van der Geest, J. H. C. Reiber, and M. Sonka, "3-D active appearance models: Segmentation of cardiac MR and ultrasound images," IEEE Trans. Med. Imaging, vol. 21, no. 9, pp. 1167–1178, Sept. 2002.
59. L. X. Gong, S. D. Pathak, D. R. Haynor, P. S. Cho, and Y. Kim, "Parametric shape modelling using deformable superellipses for prostate segmentation," IEEE Trans. Med. Imaging, vol. 23, no. 3, pp. 340–349, Mar. 2004.
60. Shen, Y. Zhan, and C. Davatzikos, "Segmentation of prostate boundaries from ultrasound images using statistical shape model," IEEE Trans. Med. Imaging, vol. 22, no. 4, pp. 539–551, Apr. 2003.
61. Shen, Z. Lao, J. Zeng, W. Zhang, I. A. Sesterhenn, L. Sun, J. W. Moul, E. H. Herskovits, G. Fichtinger, and C. Davatzikos, "Optimised prostate biopsy via a statistical atlas of spatial cancer distribution," Med. Image Anal., vol. 8, pp. 139–150, 2004.
62. J. Xie, Y. Jiang and H.-T. Tsui, "Segmentation of kidney from ultrasound images based on texture and shape priors," IEEE Trans. Med. Imaging, vol. 24, no. 1, pp. 45–57, Jan. 2005.
63. L. Fan, P. Santago, W. Riley, and D. M. Herrington, "An adaptive template-matching method and its application to the boundary detection of brachial artery ultrasound scans," Ultrasound Med. Biol, vol. 27, no. 3, pp. 399–408, Mar. 2001.
64. T. F. Cootes, C. J. Taylor, D. H. Cooper, and J. Graham, "Active shape models-their training and application," Computer Vision and Image Understanding, vol. 61, no. 1, pp. 38–59, Jan. 1995
65. T. F. Cootes, G. J. Edwards, and C. J. Taylor, "Active appearance models," in Fifth European Conf. Computer Vision, H. Burkhardt and B. Neumann, Eds., vol. 2, no. 1. Springer, Berlin, 1998, pp. 484–498.
66. Hamarneh and T. Gustavsson, "Deformable Spatio-temporal shape models: extending active shape models to 2D+time," Image Vis.

Comput., vol. 22, no. 6, pp. 461–470, June 2004.

67. M. E. Leventon, W. E. L. Grimson, and O. D. Faugeras, “Statistical shape influence in geodesic active contours.” in Conf. Comput. Vis. Pattern Recognit. Hilton Head, SC, USA: IEEE Computer Society, 2000, pp. 1316–1323.
68. J. G. Bosch, S. C. Mitchell, B. P. F. Lelieveldt, F. Nijland, O. Kamp,M. Sonka, and J. H. C. Reiber, “Automatic segmentation of echocardiographic sequences by active appearance motion models,” IEEE Trans. Med. Imaging, vol. 21, no. 11, pp. 1374–1383, Nov. 200
69. T.F Chan and L.A Vese, “Active contours without edges,” IEEE Transactions on Image Processing, vol. 10, pp. 266-277, 2001.
70. S.P.Dakua and J.A.Sahambi, " Automatic left ventricular contour extraction from cardiac magnetic resonance images using cantilever beam and random walk approach," cardiovascular engineering, vol.10, pp.30-43,2010.
71. D.L.Pham, C.Xu, J.L.Prince, “Current methods in medical image segmentation 1,” Annual review of biomedical engineering, vol.2, pp.315-337, 2000.
72. T.Chaira and S. Anand, " A Novel intuitionistic fuzzy approach for tumour/Hemorrhage detection in medical images," Journal of Scientific and Industrial Research vol.70,2011.
73. K.Zhang, L.Zhang, H.Song and D.Zhanf, " Re-Initialization free level set evolution via reaction-diffusion," IEEE Transactions on Image Processing, vol.22, pp.258-271, 2013.
74. D.Vilkomerson, S.Ricci, P.Tortoli, “Finding the peak velocity in a flow from its Doppler spectrum,” IEEE Transactions on, Ultrasonic, Ferroelectrics and frequency control, vol.60, pp.2079-2088, 2013.
75. V.Magagnin, E.Caiani, L.Delfino, C.Champlon, "Semi-Automated Analysis of Coronary flow Doppler Images: validation with manual tracings," Proceedings of IEEE International Conference on Engineering in Medicine and Biology Society, pp. 719-722, 2006.
76. S.K.Zhou, F.Guo, J.Park, “A Probabilistic, hierarchical and discriminant framework for rapid and accurate detection of deformable anatomic structure,” Proceedings of IEEE International Conference on Computer vision, pp.1-8, 2007.
77. J.Park, S.K.Zhou, J.Jackson, "Automatic Mitral valve inflow measurements from Doppler Echocardiography," Medical Image Computing and Computer-Assisted Intervention- MICCAI 2008, pp.983- 990, 2008.
78. N.Kiruthika, B.Prabhakar, M.R, Reddy, "Automated assessment of aortic regurgitation using 2D Doppler Echocardiogram," Proceedings of IEEE International Workshop Imaging Systems and Techniques on imagining read imaging, pp.95-99, 2006.
79. H.Kalinic, S.Lonkaric, M.Cikes, "Model-based segmentation of aortic ultrasound images," Proceedings of International Symposium on Image and Signal Processing and Analysis, pp.739-743, 2011.
80. T.Syeda Mahmood, P.Turaga, D.Beymer, " Shape-based similarity retrieval of Doppler images for clinical decision support," Proceedings of IEEE International Conference on Computer vision and Pattern Recognition, pp.855-862, 2010.
81. M.Agarwal, K.K.Biswas, M.Hanmandlu, "Generalised intuitionistic fuzzy soft sets with application in decision making," Applied Soft Computing, vol.13, pp.3552-3566, 2013.
82. M.Zholgharni, N.M.Dhutia, G.D.Cole, "Automated aortic Doppler flow tracing for reproducible research and clinical measurements," IEEE Transactions on Medical Imaging, vol.33, pp.1071-1082, 2014.
83. P. Bao, D. Zhang, W. Xiaonin, “Canny edge detection enhancement by scale multiplication,” IEEE Transactions on Pattern Analysis and Machine Intelligence, vol.27, pp.1485-1490, 2005.
84. T. Chiara and A.Ray, “A New Measure using intuitionistic fuzzy set theory and its application to edge detection,” Applied soft computing, vol.8, pp.919-927, 2008.
85. S.Aja Fernandez, G. Vegas Sanchez Ferrero, Fernandez, "Soft Thresholding for medical image segmentation, " Proceedings of IEEE International Conference on Engineering in Medicine and Biology Society, pp.4752-4755, 2010.
86. Larrabidi, R.Feijoo, A.Novotny, "An Image segmentation method based on a discrete version of topological derivative," In world congress structural and multidisciplinary optimisation, pp.01-11, 2005.
87. V.R. Rathod, R. Anand, A. Ashok, “Comparative analysis of NDE techniques with image processing,” Non-destructive testing and evaluation, vol.27, pp.305-326, 2012.
88. V.R. Rathod, R. Anand, "A Comparative study of different segmentation techniques for detection of flaws in nde weld images," Journal of Non-destructive evaluation, vol.31, pp.1-16, 2012.

89. J.Fu, H.C. Lien, S. Wong, "Wavelet-based histogram equalisation enhancement of gastric sonogram images," Computerised medical imaging and graphics, vol.24, pp. 59-68, 2000.
90. A. Adelkhani, B.Beheshti, S.Minaei, " Taste characterisation of orange using image processing combined with ANFIS, " Measurements, VOL.46, PP.3573-3580, 2013.
91. W.M. Hafizah, E. Supriyanto, "Automatic generation of the region of interest for kidney ultrasound images using texture analysis," International Journal of Biology and Biomedical Engineering, vol.6, pp.26-34,2012.
92. J.Alison Noble, Djamal Boukerroui, “Ultrasound Image Segmentation: A Survey,” IEEE Transactions on Medical imaging, vol.25, pp 987- 1010, 2006.
93. Donka Angelova, Lyudmila Mihaylova, “Contour segmentation in 2D Ultrasound medical images with particle filtering,” Machine vision and applications, vol.22, pp 551-561,2011.
94. Zhu, X., Huang, Z., Cheng, H., Cui, J., Shen, H.T.: Sparse hashing for fast multimedia search. ACM Transactions on Information Systems 31(2), 9 (2013) [
95. Zhu, X., Huang, Z., Cui, J., Shen, H.T.: Video-to-shot tag propagation by graph sparse group lasso. IEEE Transactions on Multimedia 15(3), 633–646 (2013)
96. Zhu, X., Huang, Z., Shen, H.T., Zhao, X.: Linear cross-modal hashing for efficient multimedia search. In: ACM Multimedia, pp. 143–152 (2013)
97. Zhu, X., Huang, Z., Tao Shen, H., Cheng, J., Xu, C.: Dimensionality reduction by mixed kernel canonical correlation analysis. Pattern Recognition 45(8), 3003–3016 (2012)
98. Zhu, X., Huang, Z., Yang, Y., Tao Shen, H., Xu, C., Luo, J.: Self-taught dimensionality reduction on the high-dimensional small-sized data. Pattern Recognition 46(1), 215–229 (2013)
99. Zhu, X., Suk, H.-I., Shen, D.: Matrix-similarity based loss function and feature selection for Alzheimer's disease diagnosis. In: CVPR, pp. 3089–3096 (2014)
100. Gyorfi, L. (1981) "The rate of convergence of k−NN regression estimates and classification rules", IEEE Trans. Information Theory, 27: 362–364.
101. Gyorfi, L. & Gyorfi, Z. (1978) "An upper bound on the asymptotic error probability of the k-Nearest Neighbor rule for multiple classes", IEEE Trans. Inform. Theory, 24: 512–514.
102. Hall, P., Park, B.U. & Samworth, R.J. (2008) "Choice of neighbour order in nearest-neighbour classification", the Annals of Statistics, 36(5): 2135-2152.
103. Hellman, M.E., (1970) "The nearest neighbour classification rule with a reject option", IEEE Trans. Systems, Man, Cybernetics, 3: 179-185.